Role of the reversible electrochemical deprotonation of phosphate species in anaerobic biocorrosion of steels

Leonardo De Silva Muñoz, Alain Bergel, Régine Basséguy

Role of the reversible electrochemical deprotonation of phosphate species in anaerobic biocorrosion of steels

Leonardo De Silva Muñoz, Alain Bergel, Régine Basséguy *

Laboratoire de Génie Chimique, CNRS-INPT, 5 rue Paulin Talabot, 31106 Toulouse, France

Received 16 February 2007; accepted 26 April 2007

Abstract

Sulphate reducing bacteria are known to play a major role in anaerobic microbiological influenced corrosion of steels, but mechanisms behind their influence are still source of debates as certain phenomena remain unexplained. Some experiments have shown that hydrogen consumption by SRB or hydrogenase increased the corrosion rate of mild steel. This was observed only in the presence of phosphate species. Here the cathodic behaviour of phosphate species on steel was studied to elucidate the role of phosphate in anaerobic corrosion of steel. Results showed: a linear correlation between reduction waves in linear voltammetry and phosphate concentration at a constant pH value; that phosphate ions induced considerable anaerobic corrosion of mild steel, which was sensitive to hydrogen concentration in the solution; and that the corrosion potential of stainless steel in presence of phosphate was shifted to more negative values as molecular hydrogen was added to the atmosphere in the reaction vessel. Phosphate species, and possibly other weak acids present in biofilms, are suggested to play an important role in the anaerobic corrosion of steels via a reversible mechanism of electrochemical deprotonation that may be accelerated by hydrogen removal.

Keywords: A. Stainless steel; A. Mild steel; C. Acid corrosion; C. Microbiological corrosion

* Corresponding author. Tel.: +33 5 34 61 52 51; fax: +33 5 34 61 52 53.
E-mail address: Regine.Basseguy@ensiacet.fr (R. Basséguy).

1. Introduction

1.1. Phosphates, SRB and hydrogenase in anaerobic biocorrosion

It has been widely demonstrated that sulphate reducing bacteria (SRB) play a major role in the anaerobic microbially influenced corrosion (MIC) of carbon steels [1–6] and stainless steels [7–9]. The mechanisms proposed to explain anaerobic MIC by SRB include: precipitation of iron sulphide, which next catalyzes proton reduction into molecular hydrogen and acts as a cathode in a galvanic couple with metallic iron [10–12]; catalysis of the reduction reaction by a hydrogenase enzyme coming from the bacteria [13]; anodic depolarization resulting from the local acidification at the anode [14]; metal ion chelating by extra cellular polymer substances (EPS) [15] and galvanic coupling with EPS [16]. Some authors have proposed oxygen as the terminal electron acceptor in a more complete model considering various effects of SRB metabolism on steel surfaces in a mixed aerobic/anaerobic system [17–21]. The old mechanism, known as cathodic depolarization, where it was assumed that the consumption of molecular hydrogen (issued from the proton or water reduction) by SRB was the rate-limiting step [22], is now considered to be wrong because hydrogen evolution on steel is an irreversible reaction [23–25]. However, experimental evidence has been provided of hydrogen removal increasing corrosion [12,26]. In these experiments, steel coupons were immerged in a phosphate solution contained in a bottle connected by the gas phase to another bottle that contained SRB. The corrosion rate increased although there was no contact between the SRB and the steel coupons, the only connection between the bottles being through the gas phase. In a similar experiment using the enzyme hydrogenase instead of SRB in the second bottle, Bryant and Laishley [27] also observed an increase in the corrosion rate of carbon steel. By using Methyl Viologen as an electron acceptor, the blue colour observed in the bottle containing hydrogenase confirmed that there was a consumption of hydrogen through the enzyme (reaction (1)).

$$H_2 + \underset{\text{(Not coloured)}}{2MV^{2+}} \xrightarrow{\text{HASE}} \underset{\text{(coloured)}}{2MV^{\cdot+}} + 2H^+ \tag{1}$$

The authors also found that the increase in corrosion rate induced by hydrogenase was possible only when the steel coupons were immersed in a solution containing phosphate ions. They proposed the following chemical reaction between steel and phosphate ions:

$$3Fe^0 + 4H_2PO_4^- \rightarrow Fe_3(PO_4)_2 + 3H_2 + 2HPO_4^{2-} \tag{2}$$

Iverson has also given evidence for the implication of phosphates in anaerobic biotic corrosion [28]. He suggests that phosphate, present in the bacterial culture medium, is reduced by some SRB strains in the presence of iron into a water soluble, volatile, corrosive, phosphorus-containing compound, may be iron phosphide (Fe_2P).

In a previous work [29] it was proved that the hydrogen atoms of the phosphate species were electrochemically reduced on stainless steel electrodes, according to the following reaction mechanism:

A two step electrochemical reduction:

$$H_2PO_4^- + e^- \leftrightarrows H_{ad} + HPO_4^{2-} \tag{3}$$

$$H_{ad} + H_2PO_4^- + e^- \leftrightarrows H_2 + HPO_4^{2-} \tag{4}$$

$$2H_{ad} \leftrightarrows H_2 \tag{5}$$

coupled with the acid–base equilibrium:

$$H_2O + HPO_4^{2-} \leftrightarrows H_2PO_4^- + OH^- \quad (6)$$

This type of reaction system is normally known as an EC′ or catalytic electrochemical–chemical mechanism [30]. It should be noted that coupling reactions (3) and (4) with the acid base equilibrium of phosphoric acid (6) leads to water reduction as the global reaction:

$$2H_2O + 2e^- \leftrightarrows H_2 + 2OH^- \quad (7)$$

The experimental data and the theoretical model proposed showed that a significant quantity of molecular hydrogen was produced by this mechanism, and the model suggested that the global reaction could be considered as reversible [29]. This reversibility may explain the influence of hydrogen removal on corrosion rate observed in the two-bottle experiments previously cited [12,26,27]. Reversible hydrogen production implies the existence of a reaction equilibrium that can be shifted if hydrogen concentration near the cathode is modified. In the case of steel corrosion in the presence of hydrogenase or SRB in solutions containing phosphate ions, the consumption of H_2 formed during the metal corrosion would increase the corrosion rate.

If phosphate species can have such an influence in the MIC of steel, other weak acids may play a similar role. Weak and strong acids are usually found in the microbial colonies or biofilms that develop on inorganic surfaces. In the case of MIC, organic acids are given an acidifying and/or chelating role [31], but there might also influence anaerobic corrosion through the reversible reduction of their hydrogen atoms similar to the mechanism proposed for phosphate.

1.2. Weak acid reduction mechanisms

The electrochemical reduction of phosphates and other weak acids on various electrodes has been the subject of several investigations [29,34–45]. The most widely accepted mechanism for the reduction of weak acids is of the CE (chemical–electrochemical) type, where the dissociation of the acid takes place before the electrochemical reduction of free protons [32–34]:

$$HA \leftrightarrows H^+ + A^- \quad (8)$$

$$2H^+ + 2e^- \leftrightarrows H_2 \quad (9)$$

The dissociation step for most weak acids is considered to be very rapid because, in most cases, no chemical limitation is found. Daniele et al. [34] propose that the limiting current obtained on platinum microelectrodes for a weak monoprotic acid depends on the concentration of both undissociated acid and free proton ([HA] and [H^+]), and on their respective diffusion coefficients (D_{HA} and D_{H+}):

$$I_L = 4Fr(D_{H^+}[H^+] + D_{HA}[HA]) \quad (10)$$

where I_L is the steady state limiting current, r is the electrode radius and F is the Faraday constant. By considering the dissociation equilibrium of the acid, Canhoto et al. [35] gives Eq. (10) the form:

$$I_L = -4\mathrm{Fr}\left(D_{H+}[H^+] + D_{HA}\frac{[H^+]}{Ka + [H^+]}C_{HA}\right) \quad (11)$$

with Ka as the dissociation constant and C_{HA} as the analytical concentration of the weak acid. This model permitted the development of electrochemical techniques for the measurement of total acid and free proton concentration in solutions of strong and weak acids [35–37]. An alternative mechanism has been proposed by other authors who claim that the hydrogen atoms of undissociated weak acids (HA) could be directly reduced without a dissociation step [29,38–40]. Stojek et al. [38] studied the influence of supporting electrolyte in the reduction of polyprotic acids on platinum electrodes. They proposed that, after the electrochemical reduction of the undissociated acid in the presence of a supporting electrolyte, the conjugate base of the acid (A^-) reacted with water or with protons (H^+) in order to re-establish the acid–base equilibrium in the solution. Marinovic et al. [39,40], using silver electrodes with citric acid and pyrophosphoric acid, have shown that weak acids could loose their hydrogen atoms via the classical CE mechanism (Eqs. (8) and (9)) or via their direct electrochemical reduction (as Eqs. (3) and (4)) and proposed some diagnostic criteria for discriminating between the two mechanisms using curves of current vs. pH at a constant potential or of potential vs. pH at a constant current. O'Neil et al. [41] and Takehara et al. [42] showed that hydrogenated phosphate species may undergo an electrochemical deprotonation on platinum electrodes. As mentioned above, we previously demonstrated the occurrence of this electrochemical deprotonation of phosphate on stainless steel and proposed a reversible reaction mechanism [29].

In order to test experimentally the reversibility of the electrochemical deprotonation of phosphate and the effect that phosphate species could have in the corrosion of carbon and stainless steels, three different types of experiments were carried out here. First, a voltammetric study was performed using stainless steel and platinum rotating disc electrodes to observe the reduction phenomena in phosphate solutions at different concentrations and pH. Then the influence of phosphate species and molecular hydrogen on the anaerobic corrosion of mild steel was observed by measuring the concentration of iron released into the solution under different H_2 partial pressures. Finally, the corrosion potential of stainless steel was measured in order to monitor its sensitivity to both hydrogen concentration and presence of phosphate species.

2. Materials and methods

2.1. Chemicals

The chemical substances used in the experiments were: dihydrogen potassium phosphate (KH_2PO_4; Prolabo), potassium chloride (KCl; Sigma Aldrich), hydrochloric acid (HCl; Acros Organics), potassium hydroxide (KOH, Prolabo), deionised water (ELGA PURELAB Option-R, 10–15 MΩ cm).

2.2. Voltammetric study

The experiments were performed in a three-electrode cell (Metrohm) using a Solartron 1286 potentiostat. The working electrode was a rotating disk made of platinum

(2 mm diameter) or AISI 316L[1] stainless steel (5 mm diameter) embedded in Teflon®. Both rotating electrodes were purchased from Radiometer. The rotation speed was controlled by a Radiometer CTV101 speed control unit. The counter-electrode was a grid made of a platinum–iridium alloy (10% iridium) and a saturated calomel electrode was used as the reference electrode (Radiometer Analytical). Experiments were carried out in solutions containing potassium chloride as the supporting electrolyte (100 mM) and different phosphate concentrations at various pH.

Before each voltammetric experiment, the working electrode was polished with a 1 μm grade abrasive sheet (3M 262x Imperial) and then ultrasonically cleaned in deionised water for 5 min. Before introducing the electrode into the cell, the solution was deoxygenated with a nitrogen gas flux for 15 min. The nitrogen flux was maintained above the solution throughout the experiment. Then, with a rotation speed of 1000 rpm, the linear voltammetry curves were drawn from −0.1 V/SCE for the platinum electrode and from −0.5 V/SCE for the stainless steel electrode to −1.1, −1.3 or −1.5 V/SCE at 20 mV/s.

2.3. Corrosion study

XC48[2] carbon steel coupons were embedded in a resin (Epofix from Struers) with only one flat face left exposed (surface area between 6 and 7 cm^2). The exposed surface was polished with abrasive paper from grade P400 to grade P4000 (LAM PLAN). The coupons were then immerged in 25 mL deoxygenated deionised water or phosphate solution. The pH of the phosphate solutions was adjusted with KOH to the pH value of the deionised water (5.7 ± 0.1). Before the immersion of the coupons, the dissolved oxygen was removed using pure nitrogen or hydrogen gas flux bubbling for 15 minutes. After at least 3 h of immersion, the concentration of the iron released in the solution was measured by ICP spectroscopy (JY-Ultima) and the coupons were examined visually.

2.4. Potentiometric study

The experiments were performed in a 50 mL closed plexiglass reactor using a Solartron 1286 potentiostat. A 316L stainless steel electrode was embedded in a resin (Combisub T 150 from Chrysor) with only one flat face left exposed (3.14 cm^2). The exposed surface was polished with abrasive paper from grade P400 to grade P4000 (LAM PLAN) and ultrasonically cleaned in deionised water for 5 min. The counter-electrode was a grid of platinum–iridium alloy (10% iridium) and a saturated calomel electrode was used as the reference electrode (Radiometer Analytical). The electrodes were immerged in 25 mL deoxygenated 100 mM KCl solution with or without 1 mM phosphate at pH = 8.0. The dissolved oxygen was removed by nitrogen bubbling in the solution for 15 min then the gas flux was left on above the solution. Potentiostatic electrolysis was performed at −0.6 V/SCE for 5 min. Then corrosion potential was plotted vs. time by measuring the open circuit potential (OCP). After each hour of measurement, the composition of the gas that flowed over the solution was modified by mixing N_2 and H_2 at atmospheric pressure using flowmeters (Sho-Rate from Brooks) to control the composition of the mixture.

[1] AISI 316L composition in percentage: C 0.03; Cr 17; Fe 65; Mn 2; Mo 2.5; Ni 12; S 0.03; P 0.045; Si 1.
[2] XC48 composition in percentage: C 0.45–0.51; $S \leqslant 0.035$; $P \leqslant 0.035$; Si 0.10–0.40; Mn 0.50–0.80.

3. Results and discussion

3.1. Voltammetric study

Linear voltammetry was performed with platinum (Fig. 1a) and stainless steel (Fig. 1b) rotating disk electrodes in 25 mL of deoxygenated solution with different phosphate concentrations (10, 50, 150, 500 mM) at pH = 8.0 and with KCl 100 mM as supporting electrolyte.

A reduction wave was observed, starting at approximately −0.7 V/SCE for the platinum (Fig. 1a) and −0.9 V/SCE for the stainless steel (Fig. 1b). For both electrodes the current density values of the waves were of the same order of magnitude with the same concentration of phosphate. The reduction current density depended strongly on phosphate concentration (Fig. 2). In Fig. 2a, the points report the current density value at −0.85 and

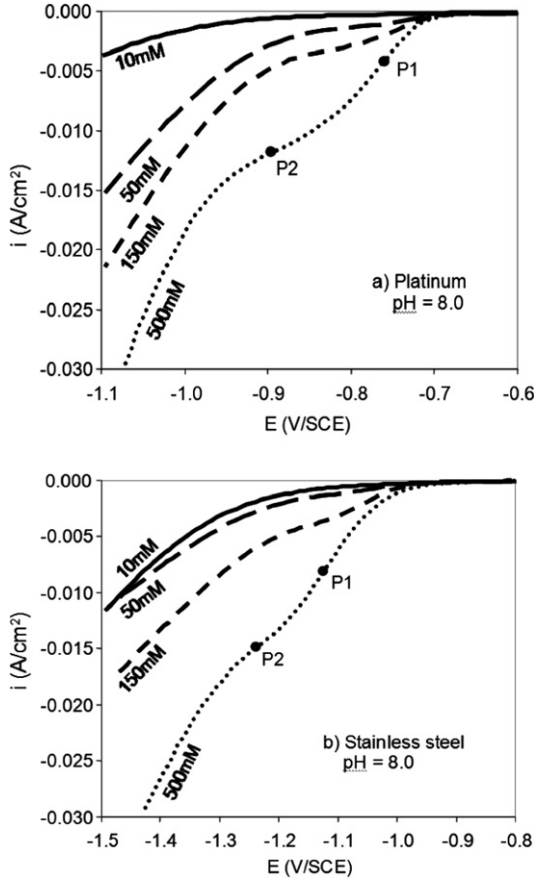

Fig. 1. Voltammetry curves (scan rate = 20 mV/s) obtained with platinum (a) and stainless steel (b) rotating disk electrodes (1000 rpm) in solutions containing different phosphate concentrations (10, 50, 150 and 500 mM) and 100 mM KCl as supporting electrolyte, pH = 8.0. The inflection points on the curves with 500 mM are marked as P1 and P2.

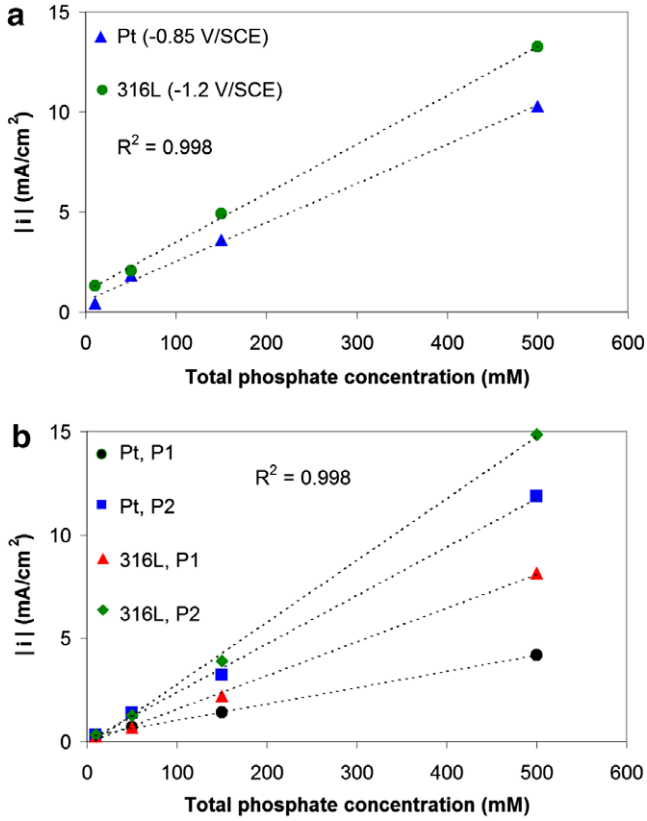

Fig. 2. (a) Current density vs. phosphate concentration at −0.85 V/SCE for platinum from Fig. 1a and at −1.20 V/SCE for 316L stainless steel from Fig. 1b. (b) Current density vs. phosphate concentration at the first (P1) and second (P2) inflection points of the waves from Fig. 1a and b for platinum and 316L stainless steel.

−1.20 V/SCE for the platinum and stainless steel electrodes respectively. In Fig. 2b, the points correspond to the current density value at the inflection points of the wave, like P1 and P2 shown in Fig. 1. The first inflection point (P1) corresponds to the initial exponential increase of the wave, and the second one (P2) is the point corresponding to the stabilisation of the wave and the starting point of the next process due to water reduction. Both approaches showed a linear relationship between current density and phosphate concentration. This linear dependency has already been observed by other authors in the steady state limiting reduction current with other weak acids such as acetic, ascorbic, monochloroacetic, lactic and HSO_4^- [43–45]. Nevertheless, the dependency between current density and weak acid concentration has not always been found to be linear [34,35] because higher acid concentration induced a higher free proton concentration (reaction (8)) and, following Eq. (11), a higher proton contribution to the reduction current [35]. However, in this work, controlling the pH of the solution avoided the occurrence of this phenomenon, and only a linear behaviour was observed in our results.

The results clearly show that the cathodic wave corresponded to the reduction of a species whose concentration was directly proportional to the phosphate content in the

solution as Daniele et al. suggested with Eq. (10) [34]. At constant pH, the increase in the cathodic current with total phosphate concentration cannot be attributed to an increase in proton concentration, which remained the same in each experiment. Furthermore at pH 8.0 the proton concentration was too small to explain the high current signal. At this pH, the predominant phosphate species involved in the reduction reaction were $H_2PO_4^-$ and HPO_4^{2-} (14% and 86% of total phosphate respectively[3]). The electrochemical reaction, which consumed hydrogen atoms of the phosphate species, perturbed the acid-base equilibrium, which was then re-established by the dissociation of water molecules, resulting in the EC′ mechanism proposed by Da Silva (reactions (3), (4) and (6)) giving:

For $H_2PO_4^-$

$$\begin{aligned} &2H_2PO_4^- + 2e^- \leftrightarrows H_2 + 2HPO_4^{2-} \\ &HPO_4^{2-} + H_2O \leftrightarrows H_2PO_4^- + OH^- \end{aligned} \tag{12}$$

and for HPO_4^{2-}

$$\begin{aligned} &2HPO_4^{2-} + 2e^- \leftrightarrows H_2 + 2PO_4^{3-} \\ &PO_4^{3-} + H_2O \leftrightarrows HPO_4^{2-} + OH^- \end{aligned} \tag{13}$$

A chemical–electrochemical (CE) mechanism may occur in the absence of supporting electrolyte where the excess negative charge at the cathode can attract protons and repel the negatively charged phosphate ions [38]. In our case however, the supporting electrolyte eliminated the charge influences on the diffusion of protons and phosphate species.

The waves observed in Fig. 1 may be attributed to diffusion controlled limitations in the reduction reaction [34], but complex reaction kinetics cannot be fully discarded. Reduction waves of this kind were also obtained in a study carried out in a thin spectro-electrochemical cell with a cell thickness from 0.24 to 0.39 mm [29]. In such a cell, diffusion limitation cannot be the cause of such behaviour. The limitation was believed to come from electrochemical kinetics of the direct reduction of the phosphate species that involved adsorption and desorption steps. Another study, using platinum microelectrodes, has indicated that the obtained limiting currents for $H_2PO_4^-$ reduction were not predictable by Eq. (10) [34] and it has been hypothesized that the dissociation step might be the limiting phenomenon.

Linear voltammetry curves were recorded with a stainless steel electrode in 150 mM phosphate solution at different pH values (Fig. 3). In general, lower pH values gave higher cathodic current intensities. At 1.0 V/SCE, the current density values were -0.7 and -38 mA/cm^2 at pH 8.0 and pH 1.5, respectively. Nevertheless the curves plotted at pH 4.0 and 6.0 were very close to each other. At these two pH values, the most abundant form of phosphoric acid was $H_2PO_4^-$ with almost the same concentration (99% of the total phosphate concentration at pH 4.0, and 94% at pH 6.0). The current obtained at pH 1.5 was much higher because, on one hand, the proton concentration was higher and could contribute significantly to the reduction current and, on the other hand, the predominant phosphate species was no longer $H_2PO_4^-$ but H_3PO_4 (82% of the total phosphate concentration). H_3PO_4 has a higher dissociation constant than $H_2PO_4^-$ ($10^{-2.16}$ for H_3PO_4 and $10^{-7.21}$ for $H_2PO_4^-$ [46]). The dissociation constant of an acid is related to the bond

[3] Calculations in Appendix.

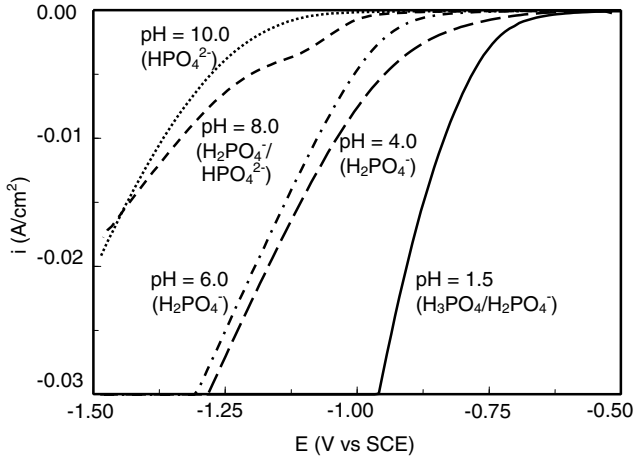

Fig. 3. Voltammetry curves (scan rate = 20 mV/s) obtained with stainless steel rotating disk electrode (1000 rpm) in solutions at different pH with 150 mM phosphate and 100 mM KCl as supporting electrolyte. Predominant phosphate species are indicated for each curve.

strength between its hydrogen atoms and the rest of the molecule. Higher dissociation constants mean weaker bond strength. This is why Daniele et al. [34] found that the reduction curves of weak acids appeared at less negative potentials as the dissociation constant of the acid increased. To illustrate the relation between the bond strength and the dissociation constant of an acid, the relationship between the Gibbs energy and the equilibrium constant of the acid base equilibrium (K_a) can be used:

$$\begin{aligned} &HA \leftrightarrows H^+ + A^- \\ &\Delta G_r^0 = -RT\ln(K_a) \end{aligned} \tag{14}$$

where ΔG_r^0 is the Gibbs energy of the reaction, R is the gas constant and T is the temperature. ΔG_r^0 would be the energy necessary to break the bond between H^+ and A^-, i.e. to dissociate HA. Comparing ΔG_r^0 values for the different phosphate species (Table 1), confirms that ΔG_r^0 is the lowest for H_3PO_4 and the highest for water. Thus, it is natural to observe lower reduction potentials with more protonated species.

Results from the voltammetric study show that the reduction of water is possible on stainless steel electrodes at a lower potential in presence of hydrogenated phosphate species. This means that phosphate and probably other weak acids can lower the

Table 1
Dissociation constants and calculated Gibbs energy for the dissociation of phosphate species and water at 25 °C and 1 atm [46]

Species	K_a	ΔG_r^0 (kJ/mol) (for $T = 25$ °C)
H_3PO_4	$10^{-2.16}$	12.33
$H_2PO_4^-$	$10^{-7.21}$	41.15
HPO_4^{2-}	$10^{-12.32}$	70.32
H_2O	$10^{-13.99}$	79.85

overpotential of the cathodic branch in the anaerobic corrosion of steel at near-neutral pH values and in this way enhance the corrosion process.

3.2. Corrosion study

Corrosion experiments were performed using mild steel coupons (XC48) submerged in phosphate solutions in different anaerobic conditions (Table 2): Constant nitrogen or hydrogen bubbling with the gas bubbles passing over the steel surface (conditions a–d); hermetically closed vessel with nitrogen or hydrogen at different pressures (conditions e–f). After at least 3 h of immersion, the iron released to the solution was measured by ICP spectroscopy.

With constant nitrogen bubbling, a carbon steel coupon was immersed in a deoxygenated 150 mM phosphate solution at pH 5.7 ± 0.1. A thick, non-conductive deposit covered the entire steel surface after 3 h of immersion (Fig. 4). This deposit may result from the precipitation of compounds made of phosphate ions and dissolved iron like vivianite ($Fe_3(PO_4)_2 \cdot 8H_2O$) or iron phosphate ($FePO_4$). These compounds are known to form a corrosion inhibiting layer on steel surfaces [47,48].

The experiment was repeated in deionised water (pH 5.7 ± 0.1). After 7 h of immersion, the iron contents in the solution of the three performed tests were 0.15, 0.17 and 0.20 mg/l (Fig. 5, condition b). In contrast, in a 0.5 mM phosphate solution, the dissolved iron concentration attained 5.62, 5.66 mg/l and a high disparate value of 10.88 mg/l (Fig. 5, condition c). When hydrogen was used instead of nitrogen, the iron concentration values were 6.18, 5.44 and 0.002 mg/l (Fig. 5, condition d). It may be concluded that, except the aberrant points of 10.88 and 0.002 mg/l, no significant difference between the use of hydrogen or nitrogen was found.

Table 2
Experimental conditions of the performed corrosion experiments

Condition name	Condition description	Medium	Immersion time (h)
a	Constant nitrogen flux in the solution over the exposed steel surface	Phosphate 150 mM, pH = 5.6	3
b	Constant nitrogen flux in the solution over the exposed steel surface	H_2O pH = 5.6	7
c	Constant nitrogen flux in the solution over the exposed steel surface	Phosphate 0.5 mM, pH = 5.8	7
d	Constant hydrogen flux in the solution over the exposed steel surface	Phosphate 0.5 mM, pH = 5.8	7
e	Closed after deoxygenating with N_2	Phosphate 0.5 mM, pH = 5.8	7
f	Pressurized at 200 kPa with H_2 after deoxygenating with H_2	Phosphate 1 mM, pH = 5.7	3
g	Pressurized at 300 kPa with H_2 after deoxygenating with H_2	Phosphate 1 mM, pH = 5.7	3
h	Pressurized at 400 kPa with H_2 after deoxygenating with H_2	Phosphate 1 mM, pH = 5.7	3
i	Pressurized at 500 kPa with H_2 after deoxygenating with H_2	Phosphate 1 mM, pH = 5.7	3

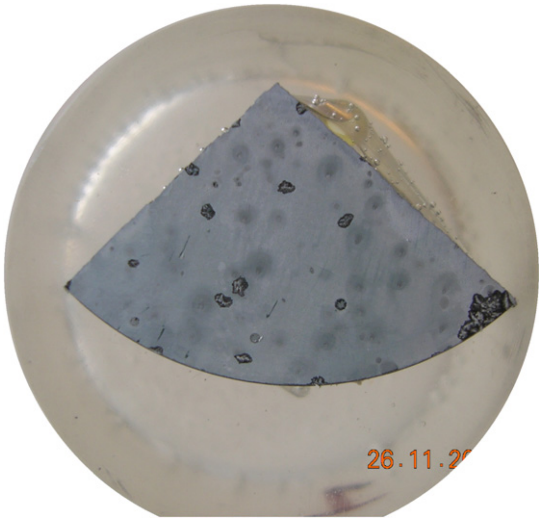

Fig. 4. Photograph of a mild steel coupon after 3 h of immersion in a deoxygenated 150 mM phosphate solution at pH = 5.6 (condition a from Table 2).

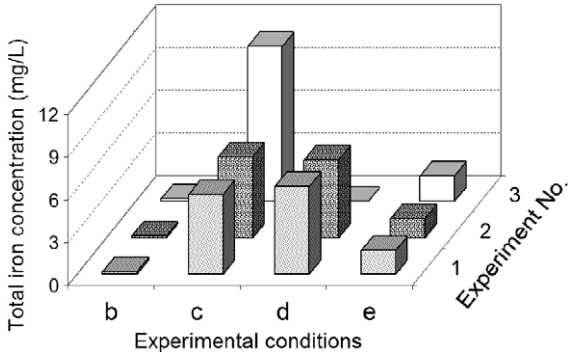

Fig. 5. Experimental values of the total iron concentration in the solution after 7 h of immersion of a mild steel coupon in four different conditions: b–e, from Table 2.

Another type of experiment was performed with the 0.5 mM phosphate solution where the vessel was kept hermetically closed after deoxygenating with N_2. The total iron concentration in the solution was considerably lower than in the case with continuous gas bubbling, attaining only 1.67, 1.34 and 1.78 mg/l (Fig. 5, condition e). An explanation for the difference of iron concentration between the conditions c and d (where constant gas bubbling was present) and condition e (where the vessel was hermetically closed) could be that bubbling removed the iron ions produced by the corrosion process from the vicinity of the steel surface and thus limited the precipitation of the protective layer (vivianite and/or iron phosphate). In this way the iron dissolution process could go on.

All the steel coupons immersed in the presence of phosphate were corroded and showed a blue-grey deposit on the steel surface, probably made of iron phosphate salts as mentioned above (Fig. 6c–e). No significant visual difference was observed between the three

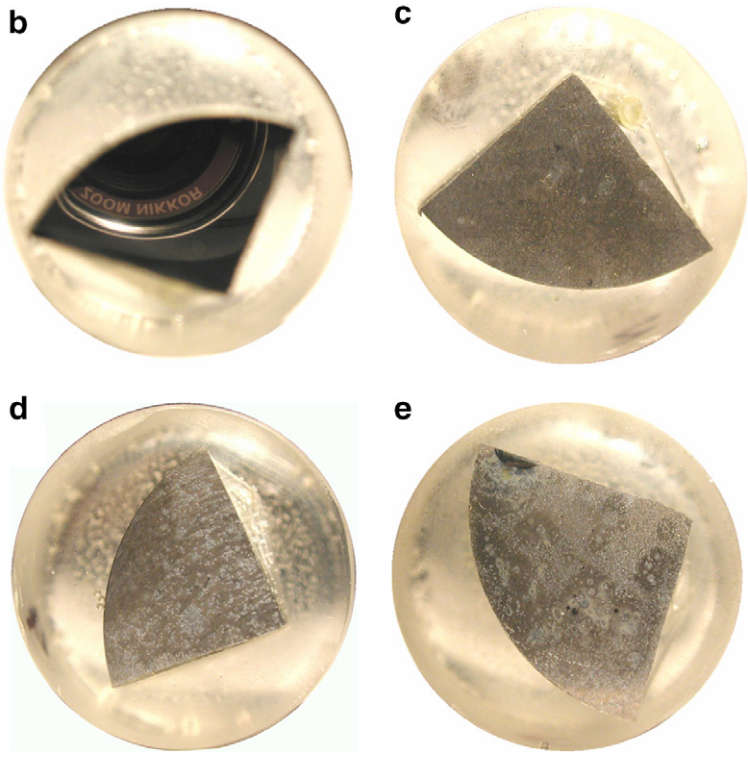

Fig. 6. Photographs of mild steel coupons after 7 h of immersion under conditions: b–e from Table 2.

corroded surfaces. In contrast, the steel coupon surface used in the absence of phosphate showed no sign of corrosion or deterioration (Fig. 6b).

Supplementary experiments were carried out in phosphate solution using pressures of hydrogen from 200 to 500 kPa (Table 2). The total iron concentration was measured after 3 h of immersion. Each condition was carried out four times (series S1, S2, S3 and S4). A higher hydrogen pressure meant a higher hydrogen content in the solution following Henry's law: $P = kC$ where P is the partial pressure (atm) of the solute above the solution, k is Henry's constant (7.8×10^{-4} l atm/mol) and C is the concentration of the solute in the solution (M). For pressures from 200 to 400 kPa, i.e. for H_2 contents from 1.5 to 3.1×10^{-3} M, the average values of the total iron concentration decreased from 1.2 to 0.5 mg/l (Fig. 7). Higher hydrogen content produced smaller corrosion rates. A higher proportion of hydrogen in the solution could shift the equilibrium (12) and (13) in the sense of the H_2 oxidation, decreasing the cathodic electron transfer rate and consequently decreasing the corrosion rate of the metal. This general behaviour was observed for each series. Nevertheless, the iron concentration obtained in the experiments carried out at 500 kPa did not follow this pattern. This may be due to an increase in the corrosion rate caused by hydrogen as has been found in some studies where hydrogen increased the corrosion rate and decreased the pitting resistance of iron and some steel alloys [49–52].

The results reported in Fig. 7 present a large dispersion in the measured iron concentration for each pressure. Actually, the iron concentration in the solution was the result

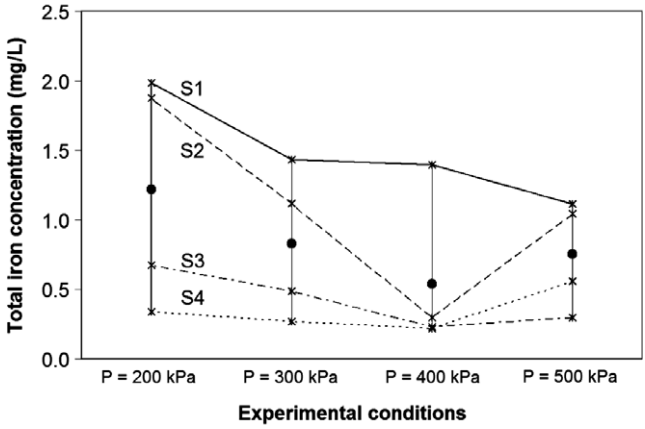

Fig. 7. Experimental (∗) and average (●) values of the total iron concentration released after a 3 h immersion of a mild steel coupon in a 1 mM phosphate solution with hydrogen gas under different pressures: 200, 300, 400 and 500 kPa (absolute) which correspond approximately to the dissoloved hydrogen concentrations of 1.5, 2.3, 3.1, 3.8 mM respectively. Four identical series of experiments were performed (S1, S2, S3 and S4).

from to two opposing phenomena: iron dissolution produced from the corrosion process and iron phosphate salt precipitation that can inhibit corrosion of the steel surface. This complex chemical system made it difficult to obtain good reproducibility among experiments. Nevertheless it should be remarked that each experiment series separately revealed exactly the same general evolution of the measured iron concentrations with the increase of hydrogen pressure.

The iron content in the solution, being an indirect measurement of the corrosion rate of the steel coupon, confirmed that the presence of phosphate, even at low concentrations and near neutral pH values, can significantly increase the corrosion rate of mild steel in anaerobic conditions and showed that this influence is sensitive to the presence of hydrogen. If the hydrogen content in the solution shifts the equilibrium of the cathodic part of the corrosion process, then the presence of hydrogen should modify the corrosion potential.

3.3. Potentiometric study

The corrosion potential of 316L stainless steel electrodes immersed in 100 mM KCl solution, with or without 1 mM phosphate, was measured under different atmospheres composed of an H_2 and N_2 mixture (Table 3). The gas mixture flowed over the solution inside the closed vessel. Starting with pure nitrogen, the composition of the mixture was changed every hour by adding hydrogen to the gas flux.

When the solution contained only KCl, the corrosion potential increased and it was not influenced by the presence of hydrogen. On the contrary, with 1 mM phosphate, the potential increased when pure N_2 was used and decreased when hydrogen was added to the gas mixture that flowed inside the cell (Fig. 8). These results show that hydrogen has an influence on the corrosion potential of stainless steel, making it less vulnerable to the corrosion process. This was possible only when phosphate species were present in the solution.

Table 3
Corrosion potential measurement experiments carried out with a 316L stainless steel electrode. F_{H_2} and F_{N_2} are the volumetric flows of hydrogen and nitrogen respectively

Condition name	Medium	$F_{H_2}/(F_{N_2}+F_{H_2}) * 100$ (1 h for each mixture)
'KCl'	KCl 100 mM pH = 8.0	0 33 66 100
'Phos-A'	Phosphate 1 mM KCl 100 mM pH = 8.0	0 33 66 100
'Phos-B'	Phosphate 1 mM KCl 100 mM pH = 8.0	0 25 50 75

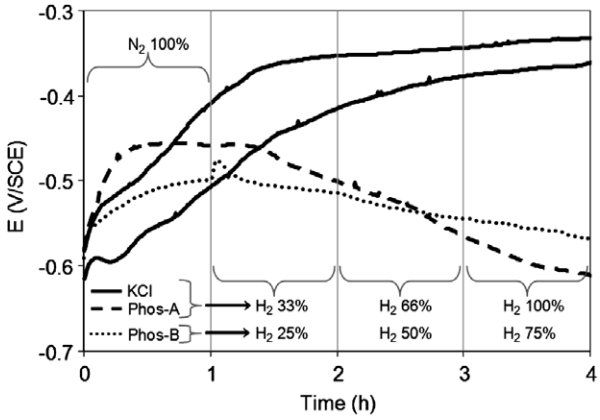

Fig. 8. Variation of the corrosion potential of stainless steel (316L) in 100 mM KCl solution ('KCl', ——) and 1 mM phosphate, 100 mM KCl solution (Phos-A, — — and 'Phos-B', ••••••) at pH 8.0 with different H_2/N_2 atmosphere mixtures (Table 3).

The decrease of the corrosion potential of stainless steel with the increase of hydrogen partial pressure is in accordance with Nernst's law applied to Eq. (12):

$$E = E^0 + \frac{RT}{2F} \ln\left(\frac{[H_2PO_4^-]^2}{P_{H_2}[HPO_4^{2-}]^2}\right) \tag{15}$$

The equilibrium potential of the reduction reaction should decrease as hydrogen concentration increases. Such an influence of hydrogen on the corrosion potential is possible only if the reduction reactions (12) and (13) are reversible. So removing hydrogen from the surface of the steel by any process (consumption via SRB respiration or hydrogenase-catalyzed oxidation, physical removal, etc.) can shift the equilibrium, in

the sense of hydrogen production, so increase the electron transfer and lead to a higher corrosion rate.

4. Conclusion

In the present work, the influence of phosphate species on the corrosion of mild steel and stainless steel was studied using linear voltammetry, open circuit potential and dissolved iron measurements. The results show that: there is a linear correlation between reduction waves and phosphate concentration at pH 8.0 observed on platinum and stainless steel electrodes; these waves correspond to the reduction of one hydrogen atom of protonated phosphate species, and the potential necessary for this reduction to occur is lower for more protonated species; phosphate ions induce considerable anaerobic corrosion of mild steel, which is sensitive to hydrogen concentration in the solution; the corrosion potential of stainless steel in presence of phosphate is shifted to more negative values as molecular hydrogen is added to the atmosphere in the reaction vessel.

All these results show that hydrogenated phosphate species play an important role in anaerobic corrosion of steels by its lower-than-water reduction overpotential and its reversible reduction mechanism. The reversibility of the cathode reaction may now clearly explain the results obtained already, particularly with the so-called two-bottle experiments [12,26,27]. These experiments have demonstrated that corrosion of steel is enhanced by the consumption of hydrogen from the gas phase by SRB or free hydrogenases contained in a second bottle. Production of hydrogen by the reversible electrochemical deprotonation of phosphate species on the steel surface is the sole hypothesis that may now fully explain these observations. The electrochemical deprotonation of phosphate introduces a new reversible cathodic reaction that sustains the hypothesis of corrosion enhancement by the consumption of molecular hydrogen. Moreover, most of the biocorrosion studies using SRB or hydrogenases have been carried out with phosphate buffer, which may significantly wander the laboratory studies from the natural conditions. These studies should now deserve revisiting. The possible similar role of weak acids that may be present in natural biofilms should also be assessed. Work is in progress in this direction.

Acknowledgements

This work has been possible thanks to the financial support of CONACYT (Mexico) and CEA-Saclay (France). Authors of this work are thankful to Dr. Damien FERON (CEA-Saclay) for his contribution to fruitful discussions.

Appendix

The abundance of the different phosphate species as a function of pH (Fig. A.1) was calculated using the phosphoric acid dissociation constants [42]:

$$K_{a1} = 10^{-2.16}$$
$$K_{a2} = 10^{-7.21}$$
$$K_{a3} = 10^{-12.32}$$

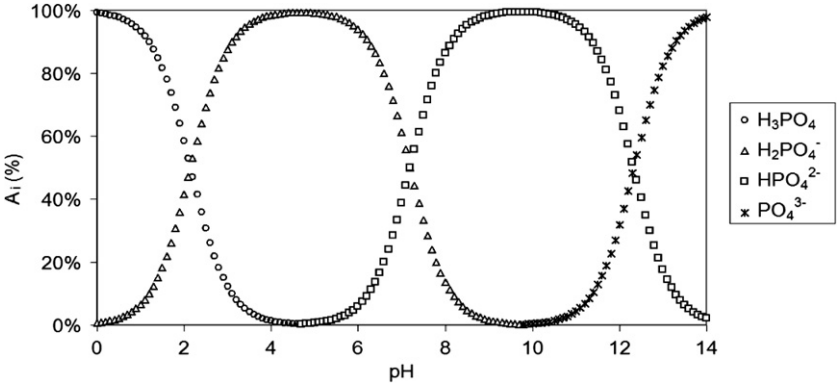

Fig. A.1. Abundance of the species i as a percentage of the total phosphate concentration vs. pH ($i = H_3PO_4, H_2PO_4^-, HPO_4^{2-}, PO_4^{3-}$).

and the equations below:

$$A_{PO_4^{3-}} = \frac{1}{\frac{[H^+]^3}{K_{a1}K_{a2}K_{a3}} + \frac{[H^+]^2}{K_{a2}K_{a3}} + \frac{[H^+]}{K_{a3}} + 1} * 100$$

$$A_{H_3PO_4} = \frac{[H^+]^3}{K_{a1}K_{a2}K_{a3}} * A_{PO_4^{3-}}$$

$$A_{H_2PO_4^-} = \frac{[H^+]^2}{K_{a2}K_{a3}} * A_{PO_4^{3-}}$$

$$A_{HPO_4^{2-}} = \frac{[H^+]}{K_{a3}} * A_{PO_4^{3-}}$$

where $[H^+]$ is the proton concentration and A_i is the abundance of the species i as a percentage of the total phosphate concentration.

References

[1] I.P. Pankhania, Biofouling 1 (1988) 27.
[2] I.T.E. Fonseca, M.J. Feio, A.R. Lino, M.A. Reis, V.L. Rainha, Electrochimica Acta 43 (1998) 213.
[3] E.S. Mc Leod, Z. Dawood, R. Mac Donald, M.C. Oosthuizen, J. Graf, P.L. Steyn, V.S. Brozel, Systematic and Applied Microbiology 21 (1998) 297.
[4] G. Chen, C.R. Clayton, Journal of Electrochemical Society 145 (1998) 1914.
[5] T.S. Rao, T.N. Sairam, B. Viswanathan, K.V.K. Nair, Corrosion Science 42 (2000) 1417.
[6] M.J. Hernández Gayosso, G. Zavala Olivares, N. Ruiz Ordaz, C. Juárez Ramirez, R. García Esquivel, A. Padilla Viveros, Electrochimica Acta 49 (2004) 4295.
[7] A.M. Brennenstuhl, T.S. Gendron, R. Cleland, Corrosion Science 35 (1993) 699.
[8] P. Angell, K. Urbanic, Corrosion Science 42 (2000) 897.
[9] J.J. Santana Rodríguez, F.J. Santana Hernández, J.E. González González, Corrosion Science 48 (2006) 1265.
[10] R.A. King, J.D.A. Miller, Nature 233 (1971) 491.
[11] R.A. King, J.D.A. Miller, British Corrosion 8 (1973) 137.
[12] B.S. Rajagopal, J. Le Gall, Applied Microbiology and Biotechnology 31 (1989) 406.
[13] S. Da Silva, R. Basseguy, A. Bergel, Journal of Electroanalytical Chemistry 561 (2004) 93.
[14] W.A. Hamilton, W. Lee, Biocorrosion, in: L.L. Barton (Ed.), Sulfate Reducing Bacteria, Plenum Press, New York, 1995, pp. 243–264.

[15] I.B. Beech, International Biodeterioration and Biodegradation 35 (1995) 59.
[16] K.Y. Chan, L.C. Xu, H.H.P. Fang, Environmental Science & Technology 36 (2002) 1720.
[17] P.H. Nielsen, W. Lee, Z. Lewandowski, M. Morrison, W.G. Characklis, Biofouling 7 (1993) 267.
[18] W. Lee, Z. Lewandowski, S. Okabe, W.G. Characklis, R. Avci, Biofouling 7 (1993) 197.
[19] W. Lee, Z. Lewandowski, M. Morrison, W.G. Characklis, R. Avci, P.H. Nielsen, Biofouling 7 (1993) 217.
[20] W. Lee, Z. Lewandowski, P.H. Nielsen, W.A. Hamilton, Biofouling 8 (1995) 165.
[21] W.A. Hamilton, Biofouling 19 (1) (2003) 65.
[22] C.A.H. Von Wolzogen Kühr, S. Van Der Vlugt, Water 18 (1934) 147.
[23] H.A. Videla, Corrosion Science 9 (1988) 585.
[24] J.L. Crolet, Matériaux et Techniques, Spécial Biocorrosion (1990) 9.
[25] J.L. Crolet, M. Magot, Materials Performance 35 (3) (1996) 60.
[26] N. Belay, L. Daniels, Antonie van leeuwenhoek 57 (1990) 1.
[27] R.D. Bryant, L. Laishley, Applied Microbiology and Biotechnology 38 (1993) 824.
[28] W.P. Iverson, Nature 217 (1968) 1265.
[29] S. Da Silva, R. Basséguy, A. Bergel, Electrochimica Acta 49 (2004) 4553.
[30] A. Molina, Journal of Electroanalytical Chemistry 583 (2005) 193.
[31] W. Sand, International Biodeterioration & Biodegradation 40 (1997) 183.
[32] J. Heyrovsky, J. Kuta, Principles of Polarography, Academic Press, New York, 1966.
[33] W.J. Albery, Electrode Kinetics, Clarendon Press, Oxford, 1975.
[34] S. Daniele, I. Lavagnini, M.A. Baldo, F. Magno, Journal of Electroanalytical Chemistry 404 (1996) 105.
[35] C. Canhoto, M. Matos, A. Rodrigues, M.D. Geraldo, M.F. Bento, Journal of Electroanalytical Chemistry 570 (2004) 63.
[36] S. Daniele, C. Bragato, M.A. Baldo, G. Mori, M. Giannetto, Analytica Chimica Acta 432 (2001) 27.
[37] S. Daniele, C. Bragato, M.A. Baldo, Electrochimica Acta 52 (2006) 54.
[38] Z. Stojek, M. Clszkowskat, J.G. Osteryoung, Analytical Chemistry 66 (1994) 1507.
[39] V. Marinović, A.R. Despić, Journal of Electroanalytical Chemistry 431 (1997) 127.
[40] V. Marinović, A.R. Despić, Electrochimica Acta 44 (1999) 4073.
[41] P. O'Neil, F. Busi, V. Concialini, O. Tubertini, Journal of Electroanalytical Chemistry 284 (1990) 59.
[42] K. Takehara, Y. Ide, T. Nakatazato, N. Yora, Journal of Electroanalytical Chemistry 293 (1990) 285.
[43] M. Ciszkowska, Z. Stojck, S.E. Morris, J.G. Osteryoung, Analytical Chemistry 64 (1992) 2372.
[44] S. Daniele, M.A. Baldo, F. Simonetto, Analytica Chimica Acta 331 (1996) 117.
[45] S. Daniele, I. Lavagnini, M.A. Baldo, F. Magno, Analytical Chemistry 70 (1998) 285.
[46] Dissociation Constants of Inorganic Species, in: David R. Lide (Ed.), CRC Handbook of Chemistry and Physics, 87th ed., Taylor and Francis, Boca Raton, FL, Internet Version, 2007.
[47] Hauke Harms et al., Corrosion Science 45 (2003) 1717.
[48] S. Da Silva, R. Basséguy, A. Bergel, Electrochimica Acta 49 (2004) 2097.
[49] H. Yashiro, B. Pound, N. Kumagai, K. Tanno, Corrosion Science 40 (1998) 781.
[50] Q. Yang, J.L. Luo, Thin Solid Films 371 (2000) 132.
[51] J.G. Yu, J.L. Luo, P.R. Norton, Electrochimica Acta 47 (2002) 1527.
[52] J.G. Yu, J.L. Luo, P.R. Norton, Electrochimica Acta 47 (2002) 401.